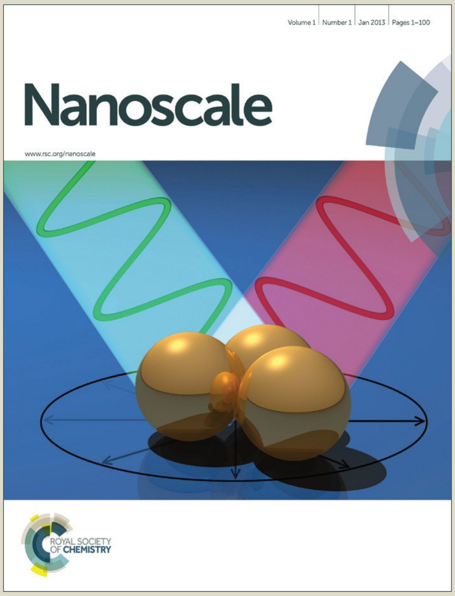

Nanoscale

ARTICLE

Graphene based anticorrosive coatings for Cr (VI) replacement

Karanveer. S. Aneja[a1], Siva Bohm[a, c*], A.S.Khanna[a2], and H.L. Mallika Bohm[b, c]

Received:
Accepted:

DOI:

www.rsc.org/

Corrosion has been a perennial issue of concern for steel industry. Chromate conversion coatings are well known pre-treatment coatings for steel but due to environmental concerns and legislations, its use and application has been restricted. The industrial community, pegged by these legislations, has been long demanding an economically viable and eco-friendly pre-treatment coating alternative, without having to compromise on the durability and corrosion performance of the overall coating system.

The present study focuses on evaluation of graphene as an anticorrosive alternative to Cr(VI) based coatings. Graphene, produced by high shear liquid exfoliation route, upon functionalisation, provides a conductive and near impermeable barrier coating. On electrochemical and coating performance evaluation of this coating system, dramatic improvement in corrosion resistance is observed. The study confirms the environmental friendly corrosion protection of steel using functionalised graphene coating.

Introduction

Steel is one of the most widely used materials today. Its areas of application include infrastructure, transport, energy, and packaging sectors [1]. To meet the global demand of steel, more than 1.6 billion tons of steel is being produced every year [1]. Despite having excellent properties like high strength, hardness, and high conductivity (electrical and thermal), steel is prone to corrosion, causing enormous economic and material loss.

Corrosion is the tendency of a metal to convert into its oxide form. The formation of oxides causes loss in properties and hence the performance of the metal. The annual cost of corrosion worldwide is estimated to be USD 2.2 trillion, which forms roughly 3% of the world's GDP [2]. Hence, a lot of efforts are being put into corrosion studies and to raise awareness about it.

Keeping in mind the bulk quantities of steel being used around the world today, the most viable and popular method of protection against corrosion is application of protective coatings. Galvanization, further strengthened by Chromium (VI) based pre-treatment layer, is widely employed as a strong protective system on both flat as well as long products of steel.

Chromium-based pre-treatments have been used quite extensively, with good success due to the fact that it can act as both cathodic (Cr^{3+}) as well as anodic (Cr^{6+}) inhibitor. They promote paint adhesion, inhibit corrosion, and are cost-effective [3]. However, due to the adverse effects of chromium (VI) on human health and environment, its use has been restricted. Environmental legislations are driving the coating industry to focus on replacing hexavalent chromium (VI) and other hazardous materials in coating systems, by next generation environment friendly materials without compromising on the coating performance.

In the past, considerable effort has gone in to develop Cr-free coating systems. Use of phosphate solutions to form a metal phosphate film was an immediate solution but requires acidic conditions for successful implementation [4]. Zirconia and Titanium based coatings, which form complex fluoro compounds, are being widely used today and have shown satisfactory performance to chromium based pre-treatments in accelerated conditions [5], but the use of fluoro based compounds is an area of concern [6]. Of late, water based coatings have begun the gain prominence. Sol–gel protective coatings has been initially demonstrated to show excellent chemical stability and enhanced corrosion resistance for metal substrates with challenges on pot life time [7].

Graphene, ever since its isolation [8] has attracted a lot of attention, both from the scientific as well as the industrial community. Owing to its phenomenal electronic and mechanical properties, it has found use in a variety of applications such as solar cells, batteries, super capacitors, flexible display touch panels, conductive inks, automobile components, etc. [9]. Protection against corrosion is one such important application. In the past few

---

[a] *Department of Metallurgical Engineering and Materials Science, IIT-Bombay, Powai, Mumbai 400076, India. Email: [1]kvsaneja@iitb.ac.in, [2]khanna@iitb.ac.in*

[b] *Tata Steel-Global wire, 16th Floor, R Tech Park Nirlon Complex, Western Express Highway, Goregaon East, Mumbai 400063, India.*
Email: mallika.bohm@wires.tatasteel.com

[c] *Tata Steel R&D-Global , Swinden Technology center, Moorgate, Rotherham, South Yorkshire S60 3AR, UK & TSL, Jamshedpur R&D Center, 831001, India.*
Email: siva.bohm@tatasteel.com

** Corresponding author*

years, efforts are on to take advantage of the properties of graphene for applications in corrosion protection of metals.

Bohm, S. [10] describes that the primary reasons for anti-corrosive applications of graphene are its high surface area, impermeable nature, and excellent electrical conductivity. Additionally, graphene and graphene based nanocomposites can be doped with corrosion inhibitors to protect the underlying metal [10] and to formulate environmentally friendly protective coatings [11]. Bohm et al. [12] incorporated graphene as a conductive coating in electrochemical fuel cell applications and demonstrated tremendous improvement against corrosion. Kirkland et al. [13] have studied electrochemical response of graphene coated nickel and copper which yielded substantial reduction in the corrosion rate. Raman et al. [14] demonstrated graphene coatings on Cu cab dramatically decrease cathodic and anodic current densities and hence retard corrosion of Cu. Dennis et al. [15] developed hybrid nanocomposite coating system that combines the electro activity of carbon nanomaterials such as multiwall carbon nanotubes (MWCNT) and exfoliated graphene with a water impermeable and high adhesive specialty polymer, polyetherimide (PEI). Potentiodynamic analysis and saltwater immersion test results indicated more than three orders of enhancement in efficiency of corrosion protection as compared with bare steel.

The major issue concerning use of graphene is the low availability of high quality graphene compounded by the high production costs. This study makes use of high shear liquid exfoliation route using distilled water as a solvent, which provides a cost effective and eco-friendly approach for graphene production [16]. Coleman et al. [17] explain the benefits of liquid exfoliation route for graphene synthesis. Paton et al. [18] describe high shear liquid exfoliation method as an industrially scalable route to produce defect free graphene flakes. Furthermore we have addressed the issue of incorporating graphene into coating system by functionalising it. This functionalised graphene formulation, when applied as a pre-treatment and coated with a primer on a cleaned mild steel substrate, leads to dramatic decrease in corrosion, which is proved in electrochemical and salt spray test results.

Experimental

2.1 Graphene Synthesis

High quality graphite (IMERYS KS 10) was added to a solution containing distilled water and surfactants [Patent in progress]. The solution was subjected to high shear mixing at 8000rpm for 8 h. The solution was further subjected to bath sonication (30 min) and centrifugation (10,000rpm for 30 min). The supernatant was separated and heated at 70˚C to obtain a concentrated graphene solution. The precipitate containing nano graphite was re-used for further graphene production.

2.2 Functionalisation of Graphene and coating application

3-(Aminopropyl)triethoxysilane (APTES), purchased from Alfa Aesar®, was hydrolysed with acidified demineralised water, and used to functionalise concentrated graphene in water solution [11, 12, 16]. The defect free graphene platelets have free electron at the edge Carbon atoms. This will attract the amino group from the APTES to form a chemical bond as shown in Figure 1. Functionalisation with APTES helps graphene build a chemical network with the metal substrate as also shown in Figure 1. Cold steel mild steel panels were cleaned by sonicating them in a bath of acetone. The formulation was then applied using a bar applicator (20 micron Wet Film Thickness) on mild steel panels. The same weight percentage of graphite was used to prepare control coating and applied on cleaned mild steel panels to evaluate the difference in their behaviour. Additionally, to compare the graphene pretreatment formulation with commercially available chromate based pretreatment, reference samples were prepared in the same manner with chromate based pretreament. Curing of these coatings was performed at 120 ºC for 90 s. However in order to improve graphene based formulation's conductivity and evaporate unwanted additives, these pretreatment coatings were further heat treated at higher temperature, i.e. 300 ºC. On complete curing of all these pretreatment coatings, a commercially available primer was applied on top of them in order to perfrom the ASTM standard tests.

2.3 Graphene Characterisation

Graphene produced was characterised using Confocal Raman Spectroscopy (Horiba HR 8000), High resolution-Transmission electron Microscopy (Joel, JEM-2100F), and Scanning Electron Microscope (Joel, JSM-7600F).

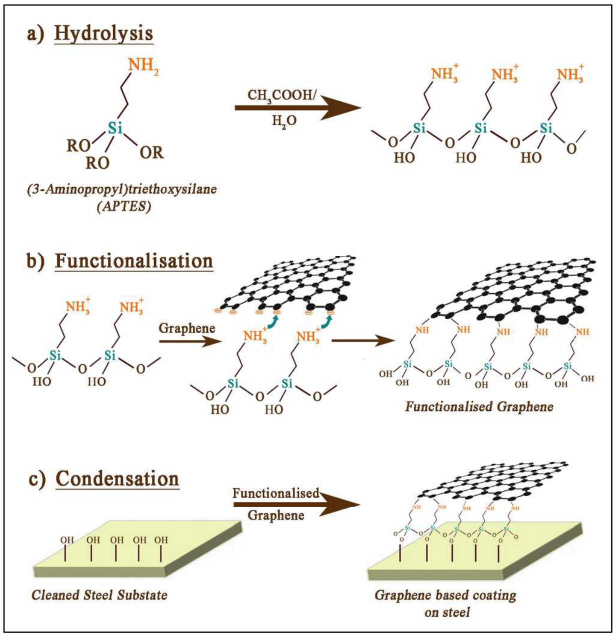

Figure 1: Schematic diagram of formulating graphene based pretreatment coating: (a) Hydrolysis of APTES with acidified demineralised water (pH 5) (b) Functionalisation of graphene (c) Application of functionalised graphene on the cleaned mild steel.

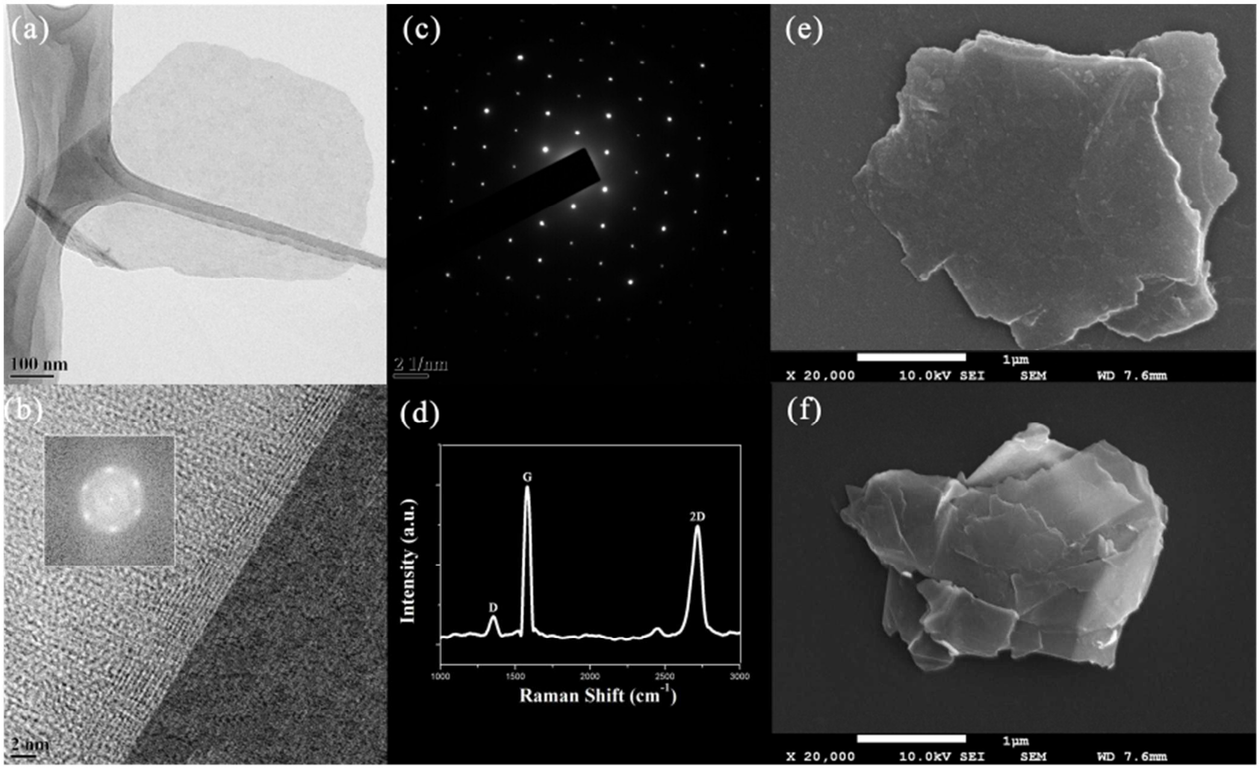

Figure 2: Graphene Characterisation (a) TEM image of a graphene flake (b) HR-TEM image of graphene and corresponding FFT image (inset). (c) Electron diffraction pattern of the produced graphene showing clearly six membered ring. (d) Raman spectra of the graphene sample (e) FEG-SEM image of graphene and (f) FEG-SEM image of graphite at the same magnification.

2.4 Structural Analysis of Graphene and Graphene based formulation

Hydrolysed APTES, graphene and graphene functionalised with hydrolysed APTES, all in powder form, were analyzed by Fourier Transform Infrared (3000 Hyperion Microscope with Vertex 80 FTIR System, Bruker, Germany). Additionally, coating cross sections were analysed using Scanning Electron Microscope (Joel, JSM-7600F) for thickness and elemental scanning.

2.5 Coating performance test

Coating performance tests were carried out according to ASTM standards to evaluate the performance of the graphene based coating system. Dry film thickness evaluation (ASTM D7091) was done to evaluate the thickness of the coating system after curing. Non-volatile matter content evaluation (ASTM D 2697) was carried out to measure the volume of dry coating obtainable from a given volume of liquid coating. Adhesion of the graphene based pretreatment was evaluated using Cross hatch tape test (ASTM D 3359). Conductivity measurement of graphene based pretreatment was carried out using four probe method (San Four Probe System-Signatone Keithley).

Corrosion performance of the coating systems was evaluated quantitatively by electrochemical techniques. Potentiodynamic polarization and electrochemical impedance spectroscopy (EIS) were performed at room temperature in 3.5% (by weight) sodium chloride (ACS Reagent) solution at pH of 5.5 and 25^{o}C. The electrochemical cell with three electrodes, where specimen (exposed area of 0.636 cm^{2}) acted as the working electrode, platinum as the counter electrode and saturated calomel electrode as the reference electrode, were employed for both the electrochemical analysis. Open circuit potential was considered to be stable when its fluctuation was less than 5mV for a period of 1000s. Impedance tests were carried out by applying a sinusoidal voltage of amplitude 10mV at the corrosion potential (E_{corr}) and responses were measured over frequencies 10mHz and 100KHz. The polarization tests were carried out in the potential range of 250mV on either side of E_{corr} and at a scan rate of 0.166 mV/s. All tests were repeated to confirm reproducibility of results.

The corrosion performance of the coating was further evaluated using Salt Fog Test (ASTM B117). Cleaned mild steel panels coated with three formulation systems, graphene based pre-treatment with commercial primer coat, graphite based pre-treatment coating with commercial primer coat, and chromium based pre-treatment

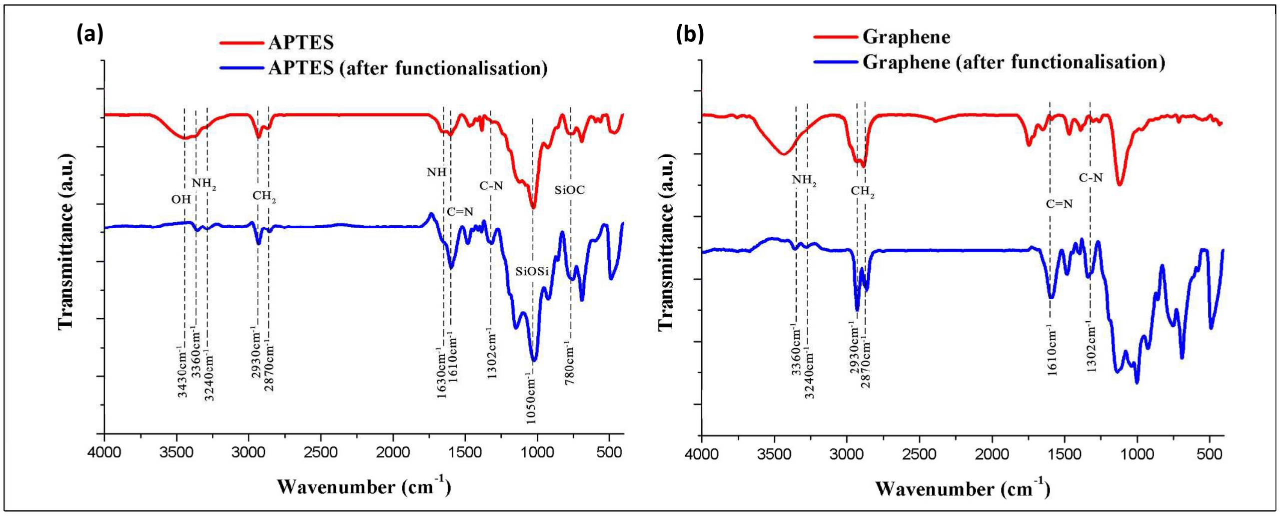

Figure 3: FTIR spectra of (a) APTES and APTES after functionalisation (b) Graphene and Graphene after functionalisation

with commercial primer were exposed in salt spray conditions as per ASTM B117 specifications i.e. the coated substrates were exposed to a salt fog chamber having 3.5wt% aqueous NaCl solution at temperature of 35±1.7 °C to evaluate their corrosion performance qualitatively.

Results

3.1 Characterisation of Graphene

D, G, and 2D characteristic peaks of graphene are observable in Raman Spectra of the produced graphene (Figure 2). A low intensity D peak corresponds to low defect concentration in the produced graphene, justifying the use of high shear liquid exfoliation for graphene production. G/2D peak intensity ratio, the shift in 2D band and the shape of the 2D peak in the Raman spectra differentiate the produced graphene from graphite [19]. This ratio is about 0.36 for monolayer and >1 for two or more layers, and increasing with the number of layers [20]. Judging by the G/2D peak intensity ratio of 1.33 in our case and the shift in 2D peak, we can conclude the number of layers to be 2 to 5 [19]. Additionally, the symmetric shape of the 2D peak confirms that after centrifugation, the supernatant contains only few layers of graphene (below 5) and no nano graphite. Also, significant increase in the surface area is evident on exfoliation of graphite by comparing the FEG-SEM images of graphite and graphene, at the same magnification.

3.2 Structural Analysis of coating

Figure 3(a) depicts FTIR spectra of APTES and graphene pre and post functionalisation. Post functionalisation APTES peaks are obtained by subtracting the graphene peaks from functionalised graphene peaks. The characteristic Si-O-Si (1050cm^{-1}) [21], Si-O-C (780cm^{-1}) [21], -CH_2 (2930cm^{-1} and 2890cm^{-1}) [22] , -NH_2 (3360cm^{-1} and 3240cm^{-1}) [22] and –NH (1630cm^{-1}) [22] peaks are visible for both curves. Significant increase in the intensity of C-N (1302 cm^{-1}) and C=N (1610 cm^{-1}) [22] peaks are observed, for post functionalisation curve. Further the changes in the fingerprint region for post functionalised APTES is an indication of the structural changes of APTES due to interaction with Graphene.

Figure 3(b) shows FTIR spectra of graphene pre and post functionalisation. The characteristic -CH_2 (2930cm^{-1} and 2890cm^{-1}) peaks are present in both curves, while, as in the case of APTES, distinct C-N (1302 cm^{-1}) and C=N (1610 cm^{-1}) peaks are observed post functionalisation providing evidence of proposed functionalisation process and formation of C-N and C=N. Again the finger print region for post-functionalised graphene differs drastically from the pre-functionalised graphene signifying chemical interaction with APTES.

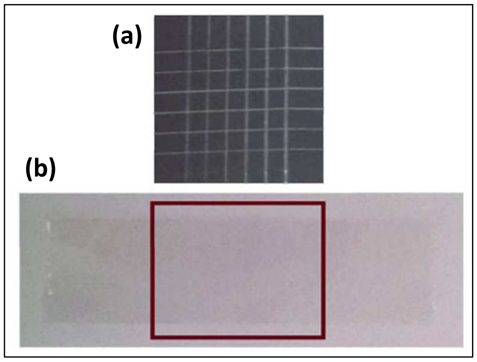

Figure 4: Cross hatch test on graphene based pre-treatment coatings (a) Sample after tape peel off (b) Tape after peel off showing no traces of coating

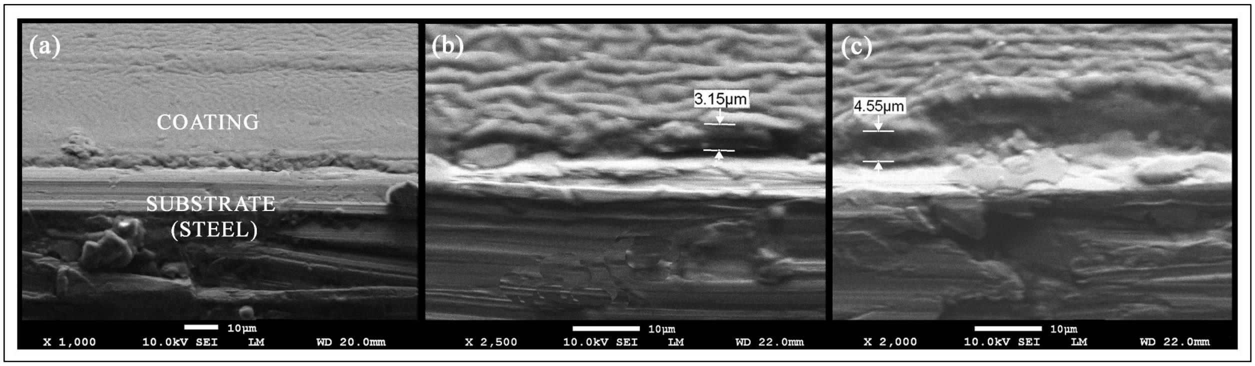

Figure 5 (a): Cross section of functionalised graphene coated steel at 1000X magnification, (b) and (c) Cross section of functionalised graphene coated steel at 2500X magnification

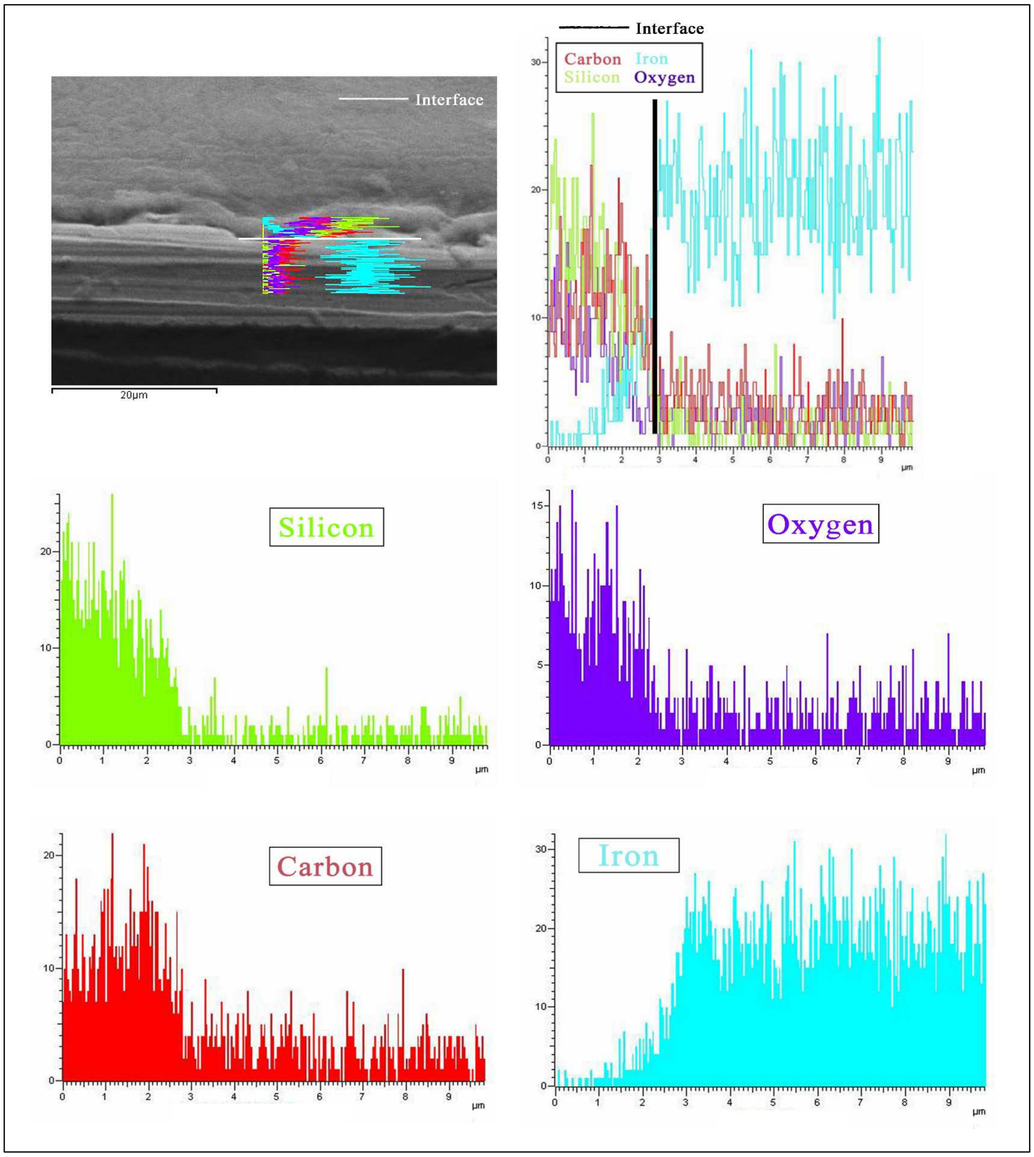

Figure 6: Line scan of graphene based pre-treatment coated sample showing distribution of various atoms along the line

The coating cross section, as shown by SEM images in Figure 5, revealed a uniform coverage of the coating. The average thickness observed was about 4 micrometre. Elemental analysis through the coating as a line scans revealed a uniform distribution of C, O and Si atoms throughout the coating thickness.

3.3.1 Dry film thickness, Adhesion and Non-volatile content

The dry film thickness, evaluated as per ASTM D7091, of the primer system was found to be 30 ± 5 µm, while that of the pre-treatment coatings was found to be less than 5 µm, as was also observed by cross sectional analysis in Figure 5. The non-volatile content in the graphene pre-treatment coating, evaluated as per ASTM D2697, was found to be 21%. Cross hatch tape test results, evaluated as per ASTM D3359, are shown in Figure 4(a) and Figure 4(b). A lattice pattern of six cuts in each direction was made. A pressure sensitive transparent tape was applied over the cut and then removed. Figure 4 (a) shows the scratched panel after tape is removed. The edges of the cuts were completely smooth and none of the squares marked were detached. Figure 4 (b) shows the tape after peeling it off and the marked area represents the area, which was attached to the coating. No traces of coating were observed on the tape. The coating showed good adhesion properties and was rated 5B as per the ASTM scale.

3.3.2 Conductivity measurement

Four probe test revealed the conductivity of the graphene to be 5 Sm^{-1} (or surface resistivity of 20 ohm cm). The high conductivity is evidence of the fact that the graphene layers produced are defect free. Additionally, high electronic conductivity of the coating may provide an alternate path for the electrons, released at the anode, to travel, thereby retarding the overall corrosion reaction [10]. Other coating systems were found to be insulating and hence did not protect the metal by this kind of mechanism.

3.3.3 Electrochemical Analysis of the developed coating systems

Figure 7 shows the potentiodynamic polarization plots for bare mild steel and mild steel with different coating systems. The corrosion potential (E_{corr}) and corrosion current density (i_{corr}) derived from the potentiodynamic polarization curves are represented in the Table 1. The corrosion potential, E_{corr}, of the graphene based coating systems was about 400mV more positive than that of the bare mild steel. It is well known that E_{corr} is the measure of corrosion susceptibility [19]. Therefore a shift in E_{corr} towards the noble side conveys the corrosion inhibiting nature of graphene. Evaluating the same system with graphite, instead of graphene, no significant shift in E_{corr} was observed, which explains the difference in roles played by graphite and graphene pigments in this coating. Tafel extrapolations of polarization curves yield corrosion current densities, which give a measure of corrosion rate in the given system. Commercially available pre-treatment and primer system provides a decrease of about two orders of magnitude in i_{corr} and corrosion rate as compared to bare mild steel. On incorporation of graphene based pre-treatment layer before the commercial primer coat, a decrease of about three orders of magnitude was found in i_{corr} and corrosion rate as compared to bare mild steel.

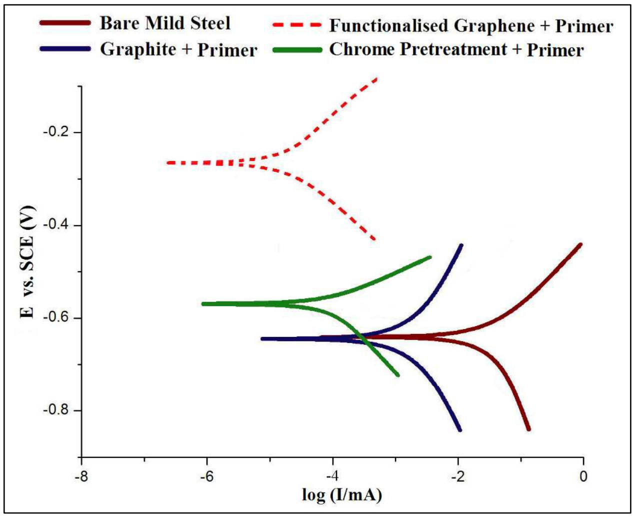

Figure 7: Polarisation plots of bare mild steel and mild steel coated different coating systems

Table 1: Potentiodynamic Polarization Parameters

COATING SYSTEM	E_{corr}(mV)	i_{corr} (µA)	Corrosion Rate (mpy)
Bare Mild Steel	-640.513	43.34	30.386
Graphite + Primer	-641.266	2.484	1.732
Chromate Pre-treatment + Primer	-563.45	0.125	0.087
Functionalised Graphene + Primer	-274.222	0.022	0.015

Electrochemical impedance studies further justify the application of graphene in protective coating systems. Bode and Nyquist plots are shown in Figure 8. In impedance studies, Z_{real} is the measure of corrosion resistance [23-25]. In Nyquist plots, Z_{real} is measured by the total diameter of the semicircle, while in Bode plots; it is the impedance value at the lowest frequency. An increase of about four orders in magnitude of Z_{real} and hence corrosion resistance is observed in case of graphene based coating system, compared to bare mild steel. The performance of graphene based system is slightly better than that of chromate based system while graphite based coating system provides only a couple of orders of improvement as compared to bare mild steel.

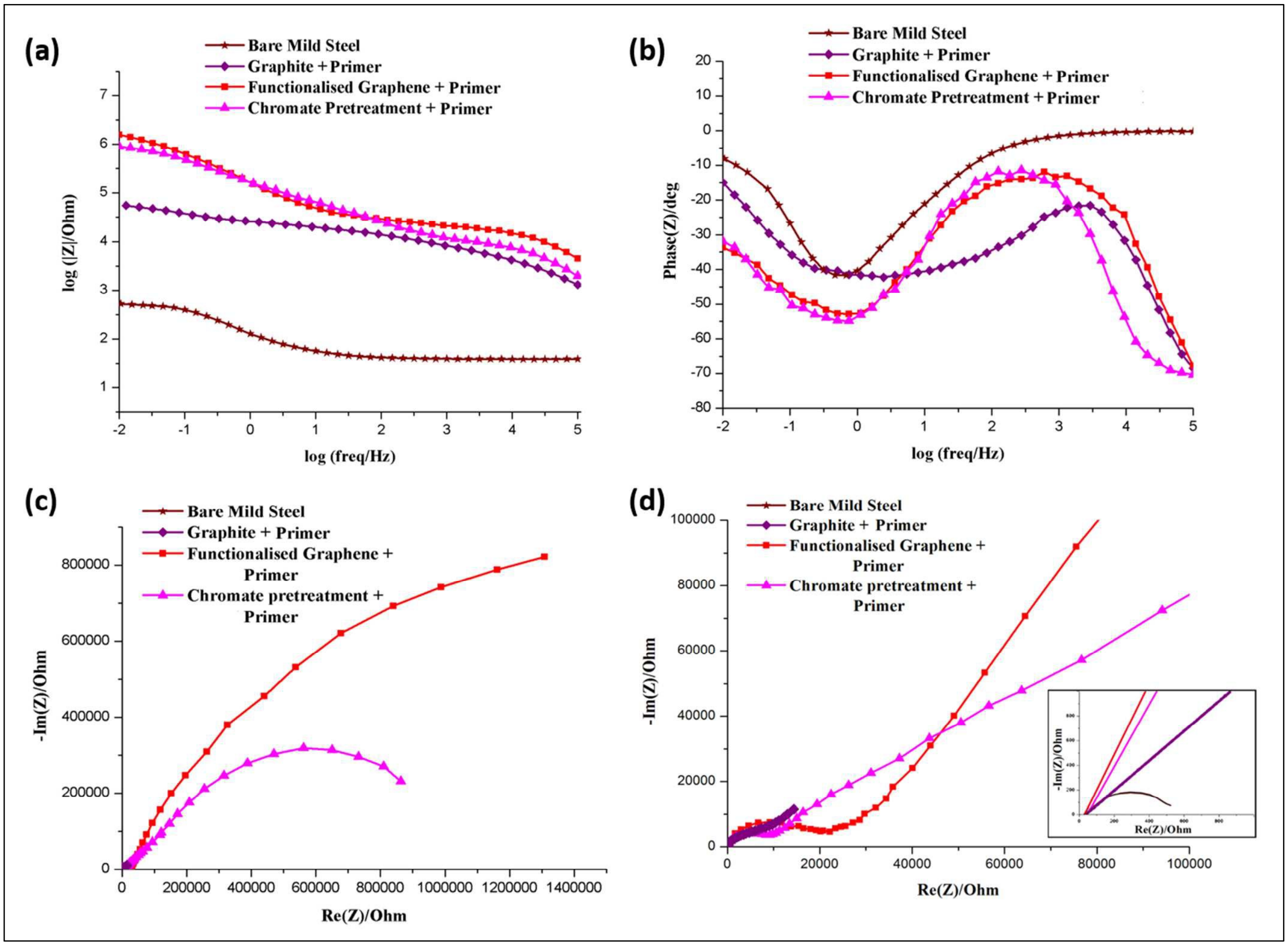

Figure 8: Electrochemical impedance study of four systems: Bare mild steel; Graphite + primer; Functionalised Graphene + primer, Chrome pre-treatment + Primer. (a) and (b) Bode plots of the four coating systems (c) and (d) Nyquist plots of the four coating systems at different scales.

A parallel combination of constant phase element (CPE) Q_f and pore resistance R_f represent the coating/solution interface, while the metal/coating interface is represented by a parallel combination of electrical double layer Q_{dl}, and charge transfer resistance R_{ct}. R_s represents the solution resistance in both the EEC models.

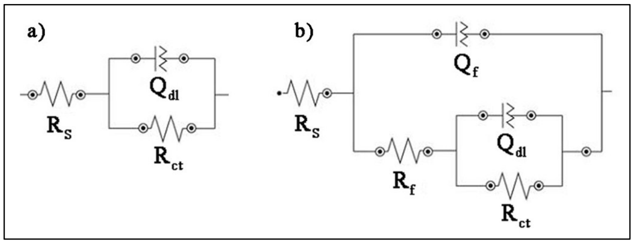

Figure 9: Electrochemical impedance modelling (a) electrochemical equivalent circuit for bare mild steel (b) Electrochemical equivalent circuit for coated mild steel systems.

These two EEC models were chosen for having the lowest percentage error (less than 7%) between the experimental and simulated data.

Comparison of the experimental and simulated data, plotted in form of Bode and Nyquist plots (Figure. 10), indicates a good degree of agreement between the two. The deviation of an interface from capacitive behaviour to that of a CPE can be attributed to the distributed surface roughness, reactivity, electrode porosity, and current and potential distributions associated with the electrode geometry [23].

Table 2. Parameters calculated using EEC in Figure 9.

Circuit Element	Bare Mild Steel	Chromate pre-treatment + Primer	Functionalised Graphene + Primer	Graphite + Primer
R_s (ohm.cm^2)	39.36	44.6	31.04	55.78
Q_f (F.s$^{(a-1)}$)	2.291×10^{-3}	1.341×10^{-9}	1.888×10^{-8}	0.288×10^{-12}
a_f	0.7068	0.961	0.6681	0.991
R_f (ohm.cm^2)	-	7320	25834	33762
Q_{dl} (F.s$^{(a-1)}$)	-	2.16×10^{-6}	1.956×10^{-6}	3.67×10^{-6}
a_{dl}	-	0.4934	0.6526	0.588
R_{ct} (ohm.cm^2)	551.6	1.645×10^6	2.813×10^6	2.069×10^5
$R_f + R_{ct}$ (ohm.cm^2)	551.6	1.652×10^6	2.838×10^6	2.406×10^5

Corrosion resistance of a given system is deduced from the mathematical sum of the R_{ct} and R_f, in case of coated mild steel systems, and the mathematical value of R_{ct} in case of bare mild steel. As evident from the analysed data from Nyquist Plot shown in Table 2, the sum of R_{ct} and R_f for the coated systems is considerably higher than R_{ct} (550 ohm cm^2) for bare mild steel. The sum is highest for graphene based coating system (approximately 2.8×10^6 ohm cm^2) followed by chromate based coating system (approximately 1.6×10^6 ohm cm^2) and lowest for the graphite based coating system (approximately 2.4×10^5 ohm cm^2). Since capacitance is directly proportional to the area of the capacitor, low values of Q_f in case of graphene based coating system compared to that of other coating systems, is a good indication of low exposure of the metal surface on incorporation of graphene into coating systems.

3.3.4 Accelerated lifetime study of coatings- Salt Spray Exposure

Salt spray test provides information about the nature of failures like blisters, rusting, cracking and delamination of film. The samples after 100, 300 and 500 hours are shown in Figure 11. Graphene based coating system remained unaffected i.e. were found to be intact and free from any defect like peeling or blisters and was capable of withstanding the corrosive environment of salt spray chamber. Mild steel panel coated with graphite based coating system underwent severe corrosion, confirming the electrochemical results that graphite increases the vulnerability of steel towards corrosion. This can be attributed to galvanic corrosion that takes place when seawater comes in contact with steel and graphite interface. A galvanic cell is formed causing rapid corrosion to take place in steel, which behaves as an anode [26]. The mild steel panel coated with chromium-based system began to corrode at the edge cut after 100 hours and suffered significant corrosion towards the end, thereby underperforming as compared to graphene pre-treated system.

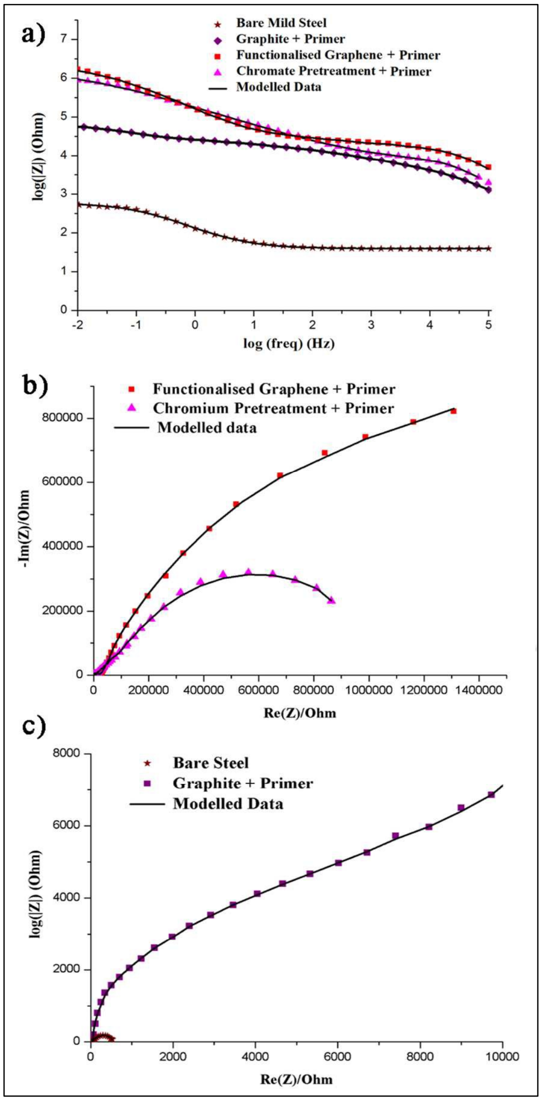

Figure 10: Comparison of experimental and modelled data in (a) Bode and (b), (c) Nyquist plots

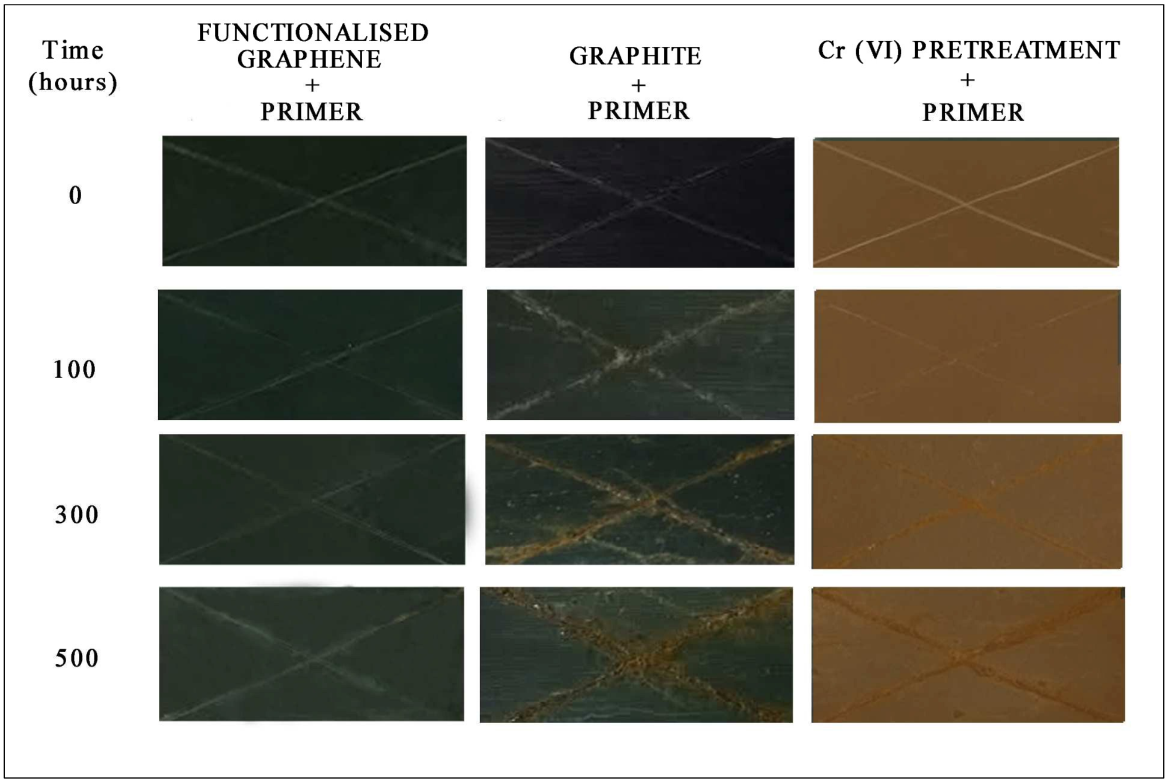

Figure 11: Salt Fog Test (ASTM B117)

Summary

Corrosion is one of the biggest challenges faced by the steel industry today. Graphene when incorporated in coating systems, provides an environmental friendly solution towards protection against corrosion. This may be attributed to three features of graphene; high surface area, impermeatbility and high conductivity. The high surface area of functionalised graphene reduces the water permeation due formation of a tortuous path. The impermeability of the graphene layer acts as a barrier to water, oxygen and other corrosive materials such as chloride, sulphates, etc. The higher conductivity achieved on graphene based coating is an indication that the coating provides an alternative path for electrons to travel, other than the metal substrate, thereby retarding the overall corrosion process. The high production cost and availability concerns surrounding graphene can be addressed by high shear liquid exfoliation route, which is an industrially scalable and economically viable solution for graphene production. This method, with the use of water as a solvent, is also environmentally friendly solution for industrial production of graphene, without having any harmful volatile content exposed to the environment. Functionalising graphene with APTES, helps incorporate graphene successfully into coating and has been demonstrated by FTIR anlaysis. The graphene based coating has been evaluated using electrochemical analysis which shows drastic improvement in anticorrosive properties. Outstanding performance of graphene based system is seen in linear polarisation studies, compared to commercially available chromate (VI) pretreatment system. In addition, salt spray results of the coating systems clearly shows that graphene significantly improves the anticorrosion properties and performs even better than chromium pre-treated system.

Conclusion

With the rising environmental concerns and chromium (VI) REACH legislations, combined with the need to sustain metals for future generations, it is the need of the hour to come up with environmental friendly and quality solutions to the corrosion menace. The use of graphene for anticorrosive application provides an eco-friendly and industrially scalable replacement to chromium (VI) based coatings. This adds a new dimension to the graphene study and opens up a wide range of applications in the coating sector.

Acknowledgement

The authors would like to thank Dr. Peter Flanagan (Imerys Graphite and Carbon) for providing graphite samples for this study. Authors would also like to acknowledge the input and help of lab collegues Dr. Swati Gaur and Mr. Siva shankar.

References

1. Steel contribution to low carbon future, Position Papers, World Steel Organisation, 2015.
2. Hays, F.G. Now is the Time. PE Director General. World Corrosion Organization
3. Deck, P.D., M. Moon, and R.J. Sujdak, *Investigation of fluoacid based conversion coatings on aluminum.* Progress in Organic Coatings, 1998. **34**(1–4): p. 39-48.
4. Chen, X.B., N. Birbilis, and T.B. Abbott, *Review of Corrosion-Resistant Conversion Coatings for Magnesium and Its Alloys.* Corrosion, 2011. **67**(3): p. 035005-1-035005-16.
5. Skar, J.I., L.K. Sivertsen, and J.M. Öster. *Chrome-free conversion coatings for magnesium die castings—a review*. in *ICEPAM–International Conference on Environmental friendly pre-treatment for Aluminum and other Metals, Oslo, Norway*. 2004.
6. Banks, R.E., B.E. Smart, and J.C. Tatlow, *Organofluorine Chemistry: Principles and Commercial Applications*. 2013: Springer US.
7. Wang, D. and G.P. Bierwagen, *Sol–gel coatings on metals for corrosion protection.* Progress in Organic Coatings, 2009. **64**(4): p. 327-338.
8. Novoselov, K.S., et al., *Electric Field Effect in Atomically Thin Carbon Films.* Science, 2004. **306**(5696): p. 666-669.
9. Ferrari, A.C., et al., *Science and technology roadmap for graphene, related two-dimensional crystals, and hybrid systems.* Nanoscale, 2015. **7**(11): Pg.no. 4587-5062.
10. Bohm, S., *Graphene against corrosion.* Nat Nano, 2014. **9**(10): p. 741-742.
11. H.L.M. BÖHM, S. BÖHM, and Van D.W.D.Hans, *Graphene based anti-corrosion coatings*, 2015, Patent no. WO 2015/090622 A1.
12. BÖHM, S., T. English, and D. Hammond, *A conductive layer for use in a photovoltaic device or other electronic application*, 2011, Patent no. WO 2011/009574.
13. Kirkland, N., et al., *Exploring graphene as a corrosion protection barrier.* Corrosion Science, 2012. **56**: p. 1-4.
14. Raman, R.S., et al., *Protecting copper from electrochemical degradation by graphene coating.* Carbon, 2012. **50**(11): p. 4040-4045.
15. Dennis, R.V., et al., *Graphene nanocomposite coatings for protecting low-alloy steels from corrosion.* American Ceramic Society Bulletin, 2013. **92**(5): p. 18-24.
16. Bohm, S. and D.H. van der WEIJDE, *Graphene based composition and graphene based coatings for electrochemical devices*, 2015, Patent no. WO 2015/074752 A1.
17. Coleman, J.N., *Liquid Exfoliation of Defect-Free Graphene.* Accounts of Chemical Research, 2013. **46**(1): p. 14-22.
18. Paton, K.R., et al., *Scalable production of large quantities of defect-free few-layer graphene by shear exfoliation in liquids.* Nat Mater, 2014. **13**(6): p. 624-630.
19. Ferrari, A.C., et al., *Raman Spectrum of Graphene and Graphene Layers.* Physical Review Letters, 2006. **97**(18): p. 187401.
20. Ni, Z., et al., *Graphene thickness determination using reflection and contrast spectroscopy.* Nano letters, 2007. **7**(9): p. 2758-2763.
21. Gaur, S., R.K. Singh Raman, and A.S. Khanna, *In vitro investigation of biodegradable polymeric coating for corrosion resistance of Mg-6Zn-Ca alloy in simulated body fluid.* Materials Science and Engineering: C, 2014. **42**: p. 91-101.
22. Wang, L., et al., *Hierarchical Nanocomposites of Polyaniline Nanowire Arrays on Reduced Graphene Oxide Sheets for Supercapacitors.* Scientific Reports, 2013. **3**: p. 3568.
23. Macdonald, J.R. and E. Barsoukov, *Impedance spectroscopy: theory, experiment, and applications.* History, 2005. **1**: p. 8.
24. Orazem, M.E. and B. Tribollet, *Electrochemical impedance spectroscopy*. Vol. 48. 2011: John Wiley & Sons.
25. Jones, D.A., *Principles and prevention of corrosion*. 1992: Macmillan.
26. Tucker, W.C., R. Brown, and L. Russell, *Corrosion between a graphite/polymer composite and metals.* Journal of Composite Materials, 1990. **24**(1): p. 92-102.